Three-dimensional optical data storage using third-harmonic generation in silver zinc phosphate glass

Lionel Canioni, Matthieu Bellec,* Arnaud Royon, Bruno Bousquet, and Thierry Cardinal

Centre de Physique Moléculaire Optique et Hertzienne, Université Bordeaux 1, 33405 Talence Cedex, France
Institut de Chimie de la Matière Condensée de Bordeaux, CNRS-Université Bordeaux 1, 87 Av. Dr. Schweitzer, 33608 Pessac, France
**Corresponding author: m.bellec@cpmoh.u-bordeaux1.fr*

Received October 8, 2007; revised December 20, 2007; accepted January 1, 2008;
posted January 9, 2008 (Doc. ID 88382); published February 13, 2008

We demonstrate the possibility of three-dimensional optical data storage inside a specific zinc phosphate glass containing silver by using third-harmonic generation (THG) imaging. Information is stored inside the glass with femtosecond laser irradiation below the refractive index modification threshold. We use the same laser for THG readout. The capability of storage with this technique is discussed. © 2008 Optical Society of America

OCIS codes: 210.0210, 210.4810.

The necessity for increasing data storage capacity, with the growth of high-density technologies, for example, requires the use of three-dimensional (3D) optically based systems. One of the methods for 3D optical data storage is based on volume holography. The physical mechanism is photochromism, which is defined as a reversible transformation of a single chemical species between two states that have different absorption spectra and refractive indices. This allows for multiplexed holographic recording and reading, such as wavelength [1], angular [2], shift [3], and phase encoding. Multiphoton bit-by-bit memory [4] is, on the other hand, another promising 3D optical data storage system, which gives rise to a higher storage density than single-photon excitation. It is based on the confinement of multiphoton absorption to a very small volume because of its nonlinear dependence on excitation irradiance. This characteristic provides a tool for activating chemical or physical processes with high spatial resolution in three dimensions. As a result there is less cross talk between neighboring data layers. Another advantage of multiphoton excitation is the use of infrared illumination, which results in the reduction of scattering and permits the recording of layers at a deep depth in a thick material. Two-photon 3D bit recording in photopolymerizable [5], photobleaching [6,7], and void creation in transparent materials [8,9] has been demonstrated with a femtosecond laser. Recording densities could reach terabits per cubic centimeter. Nevertheless, these processes suffer from several drawbacks. The index modulation associated with high bit density limits the real data storage volume due to light scattering. The fluorescence can limit the data transfer rate and the lifetime of the device. Squier and Müller anticipated third-harmonic generation (THG) for 3D data reading [9]. In this Letter, for the first time to our knowledge, we report on THG on 3D bits in a transparent material. The contrast mechanism is neither a change in refractive index nor a change in absorption, but a change in the third-order susceptibility $\chi^{(3)}$ induced by femtosecond laser irradiation in a zinc phosphate silver containing glass.

Zinc phosphate glasses are prepared for 3D data storage by a standard melting technique in a platinum crucible. The glass composition $40P_2O_5$-$5Ag_2O$-55ZnO (mol. %) allows for introducing a large amount of Ag ions without having the effect of Ag reduction. Ag solubility in phosphate glasses has been previously mentioned as well as the possibility of forming many luminescent centers without metallic particle formation after gamma irradiation for instance [10]. Details of the glass fabrication methods and the structure of the glass are available in [11]. The glass possesses an absorption cutoff wavelength at 280 nm (due to the Ag ions associated absorption at 260 nm) and emits fluorescence mainly at ~380 nm when excited at 260 nm. This intrinsic fluorescence is due to Ag^+ isolated in the glass. The prepared samples are 1 mm thick, colorless, and polished to obtain optical quality on both sides. These samples are irradiated using a femtosecond laser source emitting 440 fs, 9 MHz repetition rate pulses at 1030 nm. The laser mode is TEM_{00}, and the output polarization is TM. The maximum output average power is close to 6 W, which results in a maximum energy per pulse of 600 nJ. Acousto-optic filtering permits the tuning of the pulse energy and the repetition rate for perfect control of the accumulated effect. The femtosecond laser is focused using a reflective 36× objective with a 0.52 numerical aperture (NA) (working distance 15 mm) to a depth of 200 μm in the glass. The beam waist is estimated to be 1 μm. As shown on the experimental map sketch in Fig. 1(a), the glass is exposed to different irradiance levels (x axis) between 5×10^{12} W cm^{-2} and 10×10^{12} W cm^{-2} and a different number of pulses (y axis) from 100 to 1×10^6. The sample is manipulated through patterning of bits with a bit spacing of 20 μm using a precision xyz stage. Epiwhite light and epifluorescence microscopy are performed with com-

0146-9592/08/040360-3/$15.00

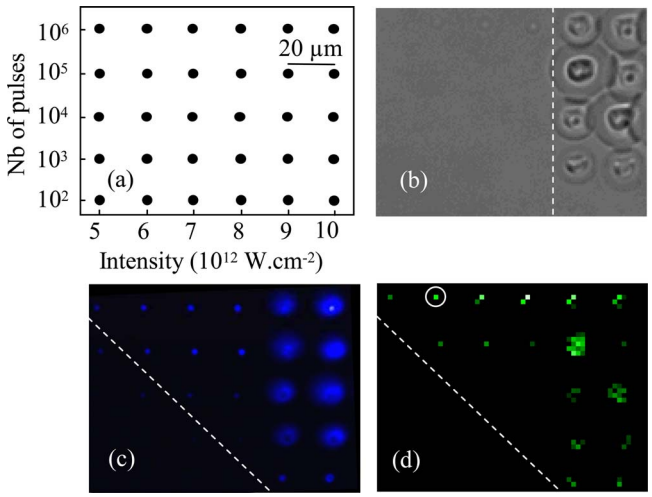

Fig. 1. (Color online) Microscopy imaging of laser-induced species following the experimental map sketch (a) (x axis, laser intensity; y axis, number of laser pulses, 6×5 bits pattern; spacing, 20 μm). (b) Epiwhite light microscopy image reveals linear refractive index modifications; vertical dashed line, damage threshold. (c) Epifluorescence microscopy image (excitation wavelength, 365 nm; emission filter, 610 ± 40 nm); slanted dashed line, threshold corresponding to induced fluorescent species. (d) THG image (excitation wavelength, 1030 nm; emission filter, 350 ± 50 nm); slanted dashed line, THG threshold; encircled area, data storage irradiation conditions ($I=6\times10^{12}$ W cm^{-2}, $N=10^6$).

mercial microscopes. A transmission confocal setup, with a 36×0.52 NA reflective objective, is used for spectroscopy and THG data collection. A UV lamp with excitation (365 nm) and emission (>400 nm) filters, and a white light source are used to obtain emission and absorption spectra. All spectra are measured using a spectrometer equipped with a CCD camera. Images are taken with a digital camera. The THG signal is collected with a photomultiplier tube and filtered by an emission bandpass filter (350 ± 50 nm). In our case, THG is excited with the same laser at low energy (<10 nJ/pulse), but, practically, a cheaper laser, such as a femtosecond fiber laser, could be used. Indeed, with a minimum energy of 0.1 nJ and an irradiance of 10^{10} W cm^{-2} (corresponding to an average power of 10 mW with a 100 MHz repetition rate), more than one third-harmonic photon by incoming pulse can be detected [12].

Transmission, fluorescence, and THG readout images of bits recorded with different irradiance levels and laser shots are presented in Figs. 1(b)–1(d), respectively. Figure 1(b) shows changes in refractive index. The damage threshold is achieved at an irradiance of 9×10^{12} W cm^{-2}, which is delimited by a vertical dashed line. At irradiances below this line, no apparent modifications are observed except for the high accumulated area in the upper part of Fig. 1(b). Nevertheless, in Fig. 1(c) we observe that fluorescence is obtained in regions where the refractive index is not modified. The same behavior is observed on the THG image in Fig. 1(d). Fluorescent and THG thresholds [the dashed slanted lines in Figs. 1(c) and 1(d)] depend not only on the laser irradiance but also on the number of pulses. For a better understanding of this dependence, spectral study (absorption and emission) of the irradiated region is performed. Figure 2(a) shows the absorbance difference between the irradiated region ($I=6\times10^{12}$ W cm^{-2}, $N=10^6$) and the nonirradiated region. An absorption band appears at ~345 nm. The emission spectrum of the fluorescent species is presented in Fig. 2(b). A band centered at 500 nm and a shoulder at 610 nm are observed. The aggregation of Ag^0 and Ag^+ ions, which generate chemically stable clusters Ag_m^{x+} (with $m<10$) explains the UV absorption and the emission spectra [13]. The formation of these clusters strongly depends on the Ag^+ mobility [10]. The accumulation of pulses induces thermal effects, which facilitate the Ag^+ diffusion [14]. This effect, associated with the Ag concentration introduced in the zinc phosphate glass (5 mol. % Ag_2O), gives rise to a high Ag cluster density. The THG image confirms that the induced Ag clusters absorb at 343 nm, corresponding to the resonant third-harmonic (3ω). Indeed, a coherent 3ω signal could be generated by each center due to the resonant absorption. The irradiated region is in the weak absorption regime and allows an enhancement of the 3ω signal [15,16]. Moreover, the image contrast is proportional to $|\chi_R^{(3)}-\chi_{NR}^{(3)}|^2$, where $\chi_R^{(3)}$ and $\chi_{NR}^{(3)}$ are the third-order susceptibilities of the irradiated (resonant) and nonirradiated (nonresonant) regions [16]. The signal is due to the electronic contribution to $\chi^{(3)}$, since only the electronic polarization is able to quickly respond to a high frequency all-optical field excitation. Therefore, at the vicinity of the nonlinear interface between the Ag clusters and the glass matrix, a coherent third-harmonic signal can be generated under femtosecond laser excitation at 1030 nm.

To demonstrate the 3D optical data storage performance according to the principle explained before, a 3D bit pattern embedded in our glass is written and read by a THG imaging setup. To achieve a high bit density in the volume, the change in refractive index must be kept as low as possible to minimize the effect of scattering of the reading beam while the change in $\chi^{(3)}$ must be as high as possible. We choose to work below the damage threshold to minimize refractive index modification and optimize creation of aggregates by the accumulated effect [the corresponding area is encircled in Fig. 1(d)]. The sample is irradiated with a laser irradiance of 6×10^{12} W cm^{-2} and

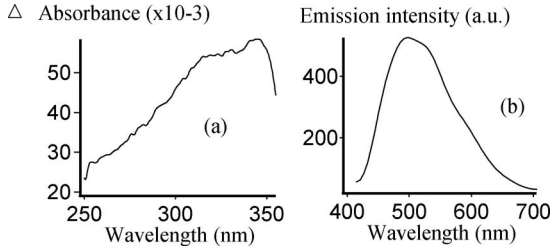

Fig. 2. (a) Differential absorbance spectrum between the irradiated and nonirradiated regions; (b) emission spectrum (excitation wavelength, 365 nm) of the irradiated region. Experimental laser irradiation conditions: $I=6\times10^{12}$ W cm^{-2}, $N=10^6$. Differential absorbance and emission spectra are assigned to laser induced Ag clusters.

with 10^6 pulses. Three layers of data are embedded 200 μm inside the sample. Each layer contains a pattern of 12×12 bits with a bit spacing of 3 μm. The letters U, B, and the numeral 1 (for University Bordeaux 1) are recorded in the first, second, and third layers, respectively, with a layer spacing of 10 μm in the z direction. As shown previously, the same laser is used for the reading procedure but with lower irradiance. By scanning the sample in xyz through the focus, the three layers (U, B, and 1) are reconstructed. As expected by the THG mechanism, an image with high contrast and no cross talk is observed in Fig. 3. Finally, the same samples were submitted to different thermal treatments below the transition temperature of the glass (T_g=375°C) at 100°C, 200°C, 300°C, 350°C during 3 h and above T_g at 400°C during 20 min. The THG signal is not modified for temperatures below T_g but disappears for temperatures higher than T_g. The recording is erased only after thermal treatment at 400°C during 20 min corresponding to a total reorganization of the glass. Then, bits could be rewritten inside the glass after polishing. Thus we can state that recording is very stable in standard conditions (up to 85°C). In our reading conditions (<10 nJ), the THG signal is not modified, even after several hours of unstopped exposure (corresponding to 10^{10} readings). Indeed, the Ag clusters are created only if enough photoelectrons are produced (threshold process). This is the reason why no modification appears during the reading process.

In this Letter, we demonstrate the possibility of 3D optical data storage inside a specific zinc phosphate glass containing Ag by using THG. The data are stored inside the glass by femtosecond laser irradiation below the refractive index modification threshold. By the accumulation effect, stable Ag clusters are created, giving rise to a formation of a nonlinear resonant interface. THG readout thus becomes possible. The main advantages of this technique compared to usual 3D data storage are no photobleaching, no change in linear refractive index, and therefore no scattering. Moreover, the THG signal is coherent and gives rise to a rather intense, directional, and less divergent beam with a high signal-to-noise ratio. Due to the fast THG response, the reading speed is limited only by the pulse duration. Finally, in our experimental conditions (bit spacing, 3 μm; layer spacing, 10 μm), 1 Gbit cm^{-3} could be stored inside the glass. Better performance can be achieved with a high NA objective (NA=1.4) even if the objective working distance limits the number of layers. According to Chen and Xie [17], the THG emission can reach radial and axial resolutions of 250 and 400 nm, respectively. Thus a storage capacity in the range of Tbits cm^{-3} is possible in our glass.

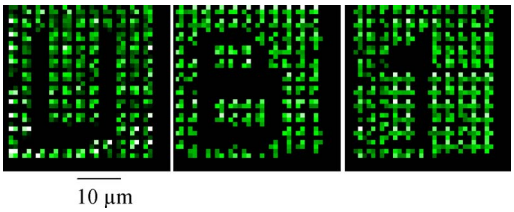

Fig. 3. (Color online) THG readout of the three layers containing the bit patterns U, B, and 1, recorded in the bulk of the glass (bit spacing, 3 μm; layer spacing, 10 μm). Laser writing parameters: $I=6\times10^{12}$ W cm^{-2}, $N=10^6$. The three THG images present high signal-to-noise ratio and no cross talk.

The authors thank P. Legros from PICIN laboratory for the use of the fluorescence microscope setup. This work was carried out with the support of a number of research equipment, and educational French and U.S. grants, including the Agence Nationale de la Recherche (ANR) (grant ANR-05-BLAN-0212-01) and the CNRS PICS grant 3179.

References

1. G. A. Rakuljic, V. Leyva, and A. Yariv, Opt. Lett. **17**, 1471 (1992).
2. F. H. Mok, Opt. Lett. **18**, 915 (1993).
3. D. Psaltis, M. Levene, A. Pu, and G. Barbastathis, Opt. Lett. **20**, 782 (1995).
4. X. Li, C. Bullen, J. W. M. Chon, R. A. Evans, and M. Gu, Appl. Phys. Lett. **90**, 161116 (2007).
5. J. H. Strickler and W. W. Webb, Opt. Lett. **16**, 1780 (1991).
6. S. Pan, A. Shih, W. Liou, M. Park, J. Bhawalkar, J. Swiatkiewicz, J. Samarabandu, P. N. Prasad, and P. C. Cheng, Scanning **19**, 156 (1997).
7. D. Day and M. Gu, Appl. Opt. **37**, 6299 (1998).
8. H. Jiu, H. Tang, J. Zhou, J. Xu, Q. Zhang, H. Xing, W. Huang, and A. Xia, Opt. Lett. **30**, 774 (2005).
9. J. A. Squier and M. Müller, Appl. Opt. **38**, 5789 (1999).
10. A. Dmitryuk, S. Parmzina, A. Perminov, N. Solov'eva, and N. Timofeev, J. Non-Cryst. Solids **202**, 173 (1996).
11. I. Belharouak, C. Parent, B. Tanguy, G. Le Flem, and M. Couzi, J. Non-Cryst. Solids **244**, 238 (1999).
12. A. Brocas, L. Canioni, and L. Sarger, Opt. Express **12**, 2317 (2004).
13. Y. Dai, X. Hu, C. Wang, D. Chen, X. Jiang, C. Zhu, B. Yu, and J. Qiu, Chem. Phys. Lett. **439**, 81 (2007).
14. V. M. Syutkin, A. V. Dmitryuk, and V. A. Tolkachev, Fiz. Khim. Stekla **18**, 66 (1992).
15. Y. R. Shen, *The Principles of Nonlinear Optics* (Wiley, 1984).
16. R. Barille, L. Canioni, L. Sarger, and G. Rivoire, Phys. Rev. E **66**, 067602 (2002).
17. J. Chen and S. Xie, J. Opt. Soc. Am. B **19**, 1604 (2002).